We are IntechOpen, the world's leading publisher of Open Access books Built by scientists, for scientists

4,800
Open access books available

122,000
International authors and editors

135M
Downloads

Our authors are among the

154
Countries delivered to

TOP 1%
most cited scientists

12.2%
Contributors from top 500 universities

WEB OF SCIENCE™

Selection of our books indexed in the Book Citation Index in Web of Science™ Core Collection (BKCI)

Interested in publishing with us?
Contact book.department@intechopen.com

Numbers displayed above are based on latest data collected.
For more information visit www.intechopen.com

20

Radiation Hardness of Semiconductor Programmable Memories and Over-voltage Protection Components

Boris Lončar[1], Miloš Vujisić[2], Koviljka Stanković[2] and Predrag Osmokrović[2]
[1]*Faculty of Technology and Metallurgy, University of Belgrade,*
[2]*Faculty of Electrical Engineering, University of Belgrade,*
Serbia

1. Introduction

The development of electronics and computer engineering, reflected particularly in the increasing degree of miniaturization and integration of electronic components, leads to their growing usage. Stability of their characteristics is very important in specific working conditions, determined by their specific implementation in different environments. These working conditions include exposure to ionizing radiation. Due to all this, a considerable amount of study and investigation is currently focused on radiation hardness of electronic components. The best indicator of this is the fact that the operation strategy of the United States Ministry of Defense states "nuclear hardness and resistive characteristics should be a part of the design, acquisition and operation of the main and auxiliary systems which perform critical missions in nuclear conflicts". From the scientific point of view, the best proof for stated claims is that each year, since 1964, USA or Canada hosts the IEEE Nuclear and Space Radiation Effects Conference (NSREC), while every two years, starting with 1991, the Radiation and Its Effect on Components and Systems Conference (RADECS) is held in Europe, at which numerous papers and workshops present results of the investigation of radiation hardness and reliability of electronic components in different working conditions and environments. Papers dealing with topics in this field are frequently cited, which is a reliable evidence of the importance of this subject.

Considering the facts stated so far, the topic of this chapter is undoubtedly in the focus of scientific interests and investigations. The chapter may be viewed as a part of a broader study of electronic components reliability, aiming to increase their radiation hardness and produce a construction design which best suits the application.

Reliability of two types of electronic components has been investigated: 1) Commercial Off the Shelf (COTS) semiconductor programmable memories (EPROM and EEPROM); and 2) over-voltage protection elements (transient voltage suppression diodes (TVS diodes), metal-oxide varistors (MOVs), gas-filled surge arresters (GFSA) and polycarbonate capacitors).

Source: Micro Electronic and Mechanical Systems, Book edited by: Kenichi Takahata,
ISBN 978-953-307-027-8, pp. 572, December 2009, INTECH, Croatia, downloaded from SCIYO.COM

2. Radiation hardness of programmable memories

2.1 Theory

Reliability of programmable memories is of great importance due to their widespread application in electronic devices. When hardness design of these components is not efficient enough, radiation effects can cause their partial damage or complete destruction.

Major advantages of Electrically Erasable Programmable Read Only Memory (EEPROM) over Erasable Programmable Read Only Memory (EPROM) components are the elimination of UV erase equipment and the much faster in-the-system erasing process (in milliseconds compared with minutes for high-density EPROM). On the other hand, a major drawback of EEPROMs is the large size of their two transistor memory cells compared to single transistor cells of EPROMs (Prince, 1991). Following the shift from NMOS to CMOS transistor technology, presentday programmable non-volatile memories are mostly CMOS-based, as is the case with both memory models investigated in this paper. Since EPROM and EEPROM cells utilize a similar floating gate structure, their radiation responses are similar as well.

The influence of neutron displacement damage, reflected in the change of minority carrier lifetime, is negligible in all MOS (Metal-Oxide Semiconductor) structures, since they are majority carrier devices. Other types of neutron damage, including secondary ionization and carrier removal, are minimal and indirect (Ma & Dressendorfer, 1989).

CMOS is naturally immune to alpha radiation, due to the shallow well. The formation of electron-hole pairs by an alpha particle will primarily take place in the substrate below the well. The well forms an electrical barrier to the carriers, preventing them from reaching the gate and influencing transistor operation. Any carriers generated in the well itself recombine quickly or get lost in the flow of majority carriers (Srour, 1982).

Gamma radiation may cause significant damage to programmable memories, deteriorating properties of the oxide layer, and was therefore considered in this chapter.

2.2 Experimental procedure

Examination of EPROM and EEPROM radiation hardness was carried out in cobalt-60 (^{60}Co) gamma radiation field. Absorbed dose dependence of the changes in memory samples caused by irradiation was monitored.

The ^{60}Co source was manufactured at Harwell Laboratory. Air kerma rate was measured at various distances from the source with a Baldwin-Farmer ionization chamber. Absorbed dose was specified by changing the duration of irradiation and the distance between the source and the examined memory samples. Absorbed dose in Si was calculated from the absorbed dose in air, by using the appropriate mass energy-absorption coefficients for an average energy of ^{60}Co gamma quanta equal to 1.25 MeV. Mass energy-absorption coefficients for silicon (μ_{enSi}(1.25 MeV) = 0.02652 cm^2/g) and air (μ_{enAIR}(1.25 MeV) = 0.02666 cm^2/g) were obtained from the NIST tables (Hubell & Seltzer, 2004).

Testing was performed on samples of COTS EPROMs and EEPROMs. EPROMs used for the investigations were NM27C512 8F85 components, with 64 KB storage capacity, packaged in a DIP 28 chip carrier. EEPROM samples used were M24128 - B W BN 5 T P, with 16 KB storage capacity, packaged in a PDIP 8 chip carrier. Fifty samples were used for both EPROM and EEPROM testing, from which the average results presented in the paper were obtained. All tests were performed at room temperature (25^{o}C). Irradiation of a 50-sample batch was conducted in consecutive steps, corresponding to the increase of total absorbed dose. Dose increment was 20 Gy per irradiation step for EPROMs and 60 Gy for EEPROMs.

All memory locations (cells) were initially written into a logic '1' state, corresponding to an excess amount of electron charge stored on the floating gate. This state has been shown to be more radiation sensitive than the '0' state, responding with a greater threshold voltage shift for the same absorbed dose. (Snyder et al., 1989). Effects of gamma radiation were examined in terms of the number of "faults" in memory samples following irradiation. A fault is defined by the change of a memory cell logic state as a consequence of irradiation. The content of all memory locations was examined after each irradiation step, whereby the number of read logic '0' states equaled the number of faults.
Although ionizing radiation effects in MOS structures are generally dose-rate dependent, effects in EPROM and EEPROM cells don't depend on dose rate. Radiation induced charge changes on the floating gate occur extremely fast, and so are in phase with any incident radiation pulse (Lončar et al., 2001).

2.3 Experimental results and discussion

Both the differential and aggregate relative change of the number of faults with the absorbed dose in EPROM samples is shown in Fig. 1 a) and b). These plots were obtained as an average over the results for all 50 samples, and the corresponding statistical dispersion is presented in Fig. 1 c). First faults, of the order of 0.1%, appeared at 1220 Gy. The number of faults increased with the rise of the absorbed dose. At dose values above 1300 Gy, significant changes in memory content were observed.
Changes in EPROMs proved to be reversible, i.e. after UV erasure and reprogramming all EPROM components became functional again - consecutive erasing, writing and reading of the previously irradiated samples was efficiently performed several times.
A repeated irradiation procedure of EPROM samples, following erasure and reprogramming to '1' state, produced faults already at 80 Gy, with significant failures in memory content occurring above 130 Gy, as shown in Fig. 2 a) and b). The lower threshold of fault occurrence upon repeated irradiation shows evidence of the cumulative nature of radiation effects. Fig. 2 c) presents the corresponding statistical dispersion.
The differential and aggregate relative change of the number of faults with the absorbed dose in irradiated EEPROM samples is shown in Fig. 3 a) and b). The plots were obtained as an average over all 50 samples used, and the corresponding statistical dispersion is presented in Fig. 3 c). First faults appeared at 1000 Gy, proving EEPROMs to be more sensitive to gamma radiation than EPROM components. With further dose increase, the number of faults also increased. Moreover, the changes in EEPROMs appeared to be irreversible. Irreversibility of radiation damage in EEPROMs was established based on the fact that the standard erasure procedure was unable to erase the contents of any of the irradiated memory samples. In CMOS EPROMs and EEPROMs, utilizing either N-well or P-well technology, the dual polysilicon gate, consisting of the control and the floating gate, resides over an N-channel transistor. Polysilicon layer floating gate, insulated from the control gate above it and the silicon channel below it by the gate oxide, is used to store charge and thus maintain a logical state. Charge is stored on the floating gate through hot electron injection from the channel in EPROMs, and through cold electron tunneling from the drain in EEPROMs. The stored charge determines the value of transistor threshold voltage, making the memory cell either 'on' or 'off' at readout (Vujisić a et al., 2007).

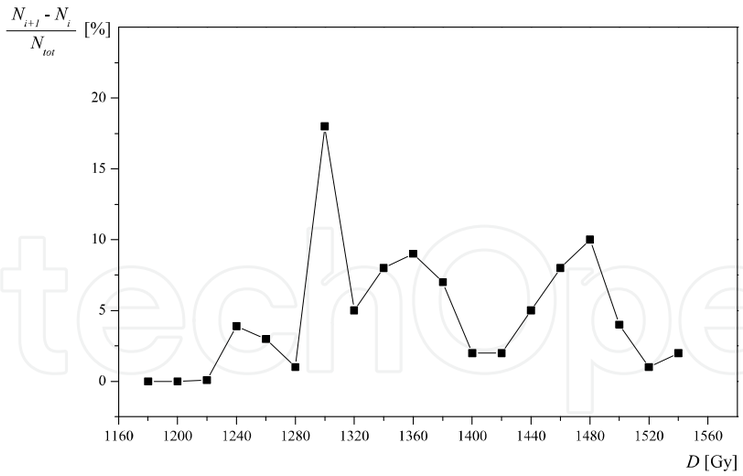

(a)

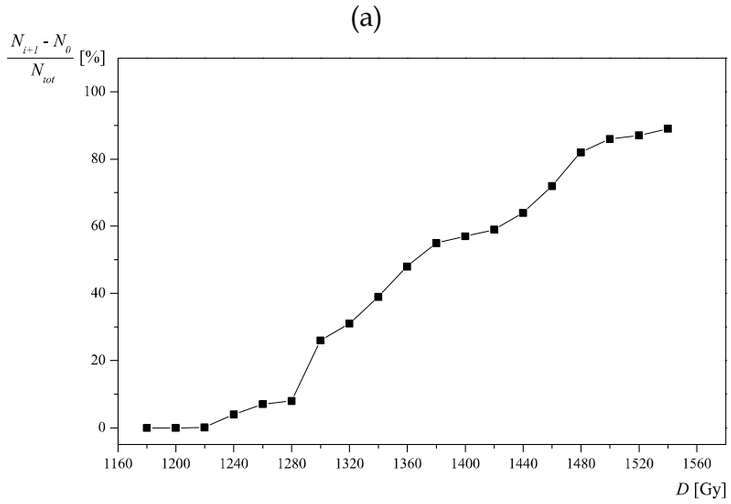

(b)

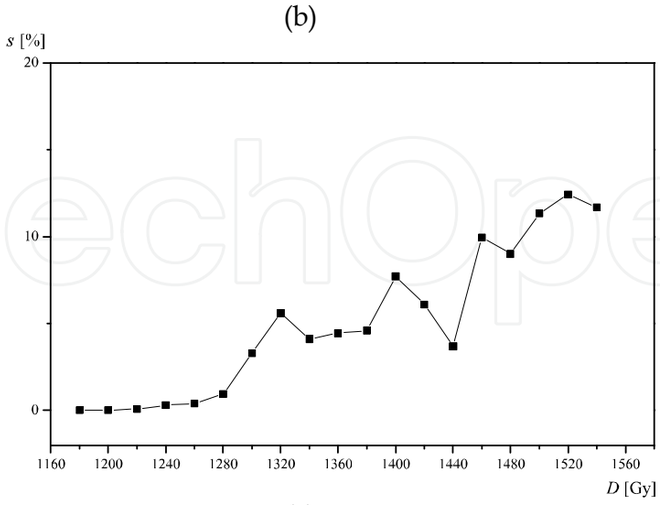

(c)

Fig. 1. Average relative change of the number of faults with absorbed dose in irradiated EPROM samples: a) differential, b) aggregate (N_{tot} = 512 bits, N_0 = 0), c) corresponding statistical dispersion.

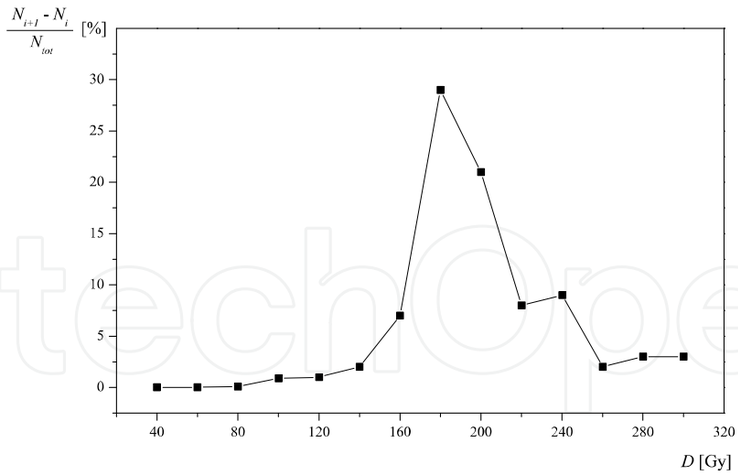

(a)

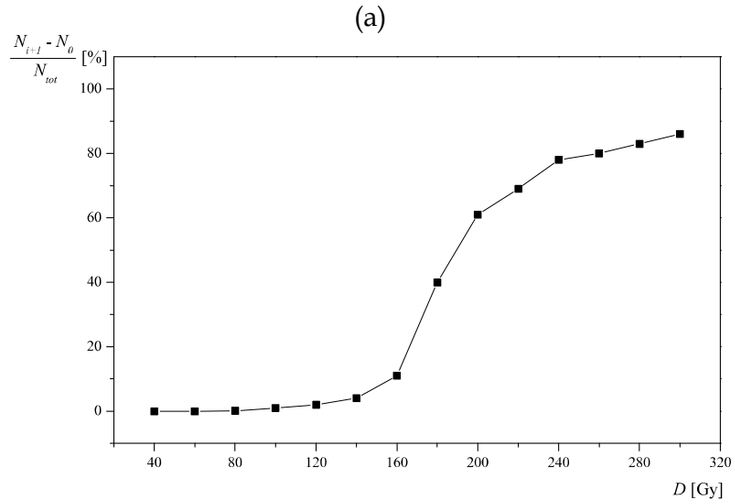

(b)

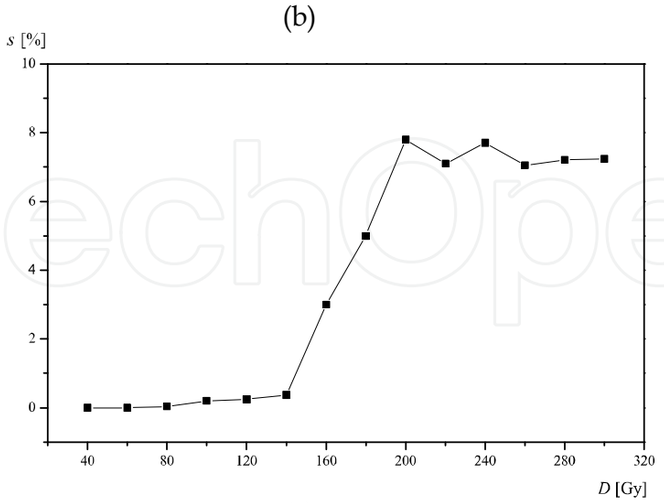

(c)

Fig. 2. Average relative change of the number of faults with absorbed dose in reprogrammed and repeatedly irradiated EPROM samples: a) differential, b) aggregate (N_{tot} = 512 bits, N_0 = 0) ,c) corresponding statistical dispersion.

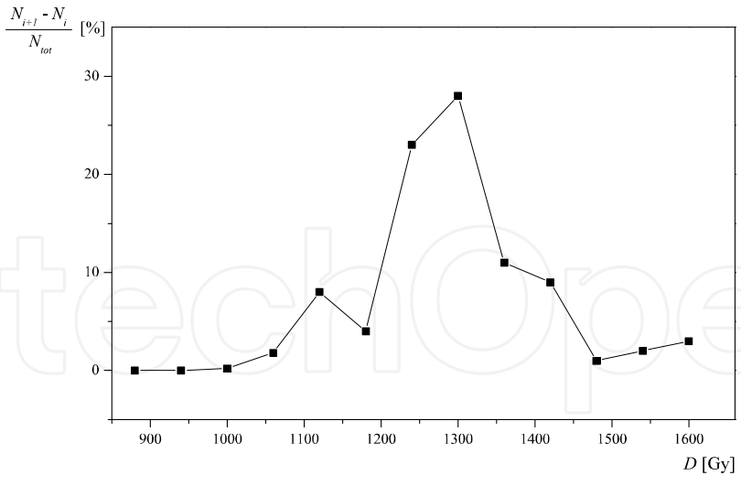

(a)

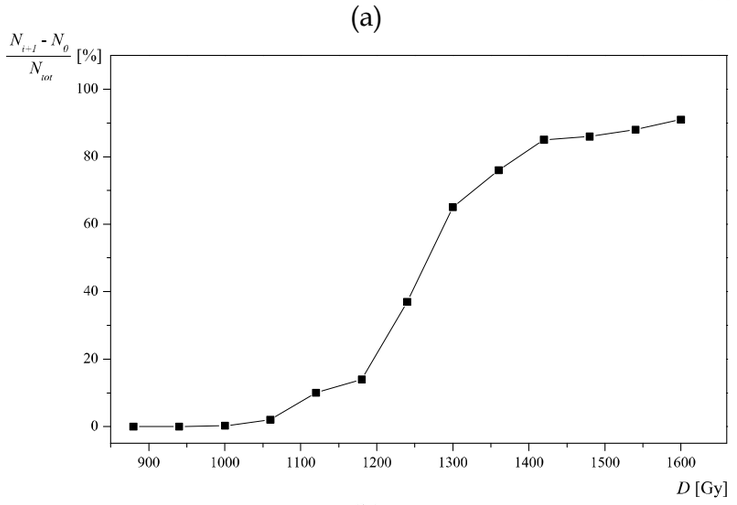

(b)

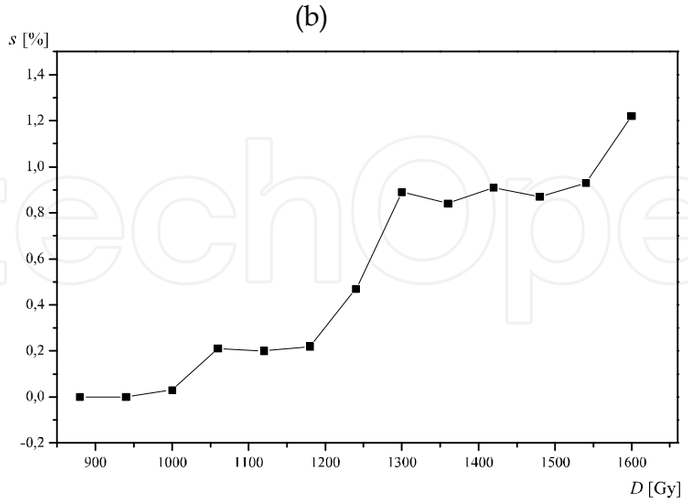

(c)

Fig. 3. Average relative change of the number of faults with absorbed dose in irradiated EEPROM samples: a) differential, b) aggregate (N_{tot} = 128 bits, N_0 = 0), c) corresponding statistical dispersion.

Passing through the gate oxide (SiO_2), gamma radiation breaks Si−O and Si−Si covalent bonds, creating electron/hole pairs. The number of generated electron/hole pairs depends on gate oxide thickness. Recombination rate of these secondary electrons and holes depends on the intensity of electric field in the irradiated oxide, created by charge trapped at the floating gate, and modulated by the change in charge carrier concentration and their separation within the oxide. The greater the electric field, the larger the number of carriers evading recombination. Incident gamma photons generate relatively isolated charge pairs, and recombination is a much weaker process than in the case of highly ionizing particles.

Secondary electrons which escape recombination are highly mobile at room temperature. In the '1' state of the memory cell, excess amount of electrons stored on the floating gate maintains an electric field in both oxide layers, that swiftly drives the secondary electrons away from the oxide to the silicon substrate and the control gate. While traversing the oxide, radiation-generated secondary electrons themselves create additional electron/hole pairs. Some of the secondary electrons may be trapped within the oxide, but this is a low-probability event, due to their high mobility and the low concentration of electron trapping sites in SiO_2 (Ristić et al., 1998).

In addition to electron/hole pair creation, secondary electrons may produce defects in the oxide by way of impact ionization. Colliding with a bonded electron in either an unstrained silicon-oxygen bond (≡Si−O−Si≡), a strained silicon-oxygen bond, or a strained oxygen vacancy bond (≡Si−Si≡), a secondary electron may give rise to one of the hole trapping complexes. Interaction with a unstrained silicon-oxygen bond gives rise to one of the energetically shallow complexes (≡Si−O•.$^{+}$Si≡ or ≡Si−O^{+}.•Si≡, where • denotes the remaining electron from the bond). Strained silicon-oxygen bonds, distributed mainly near the oxide/substrate and oxide/floating gate interfaces, are easily broken by the passing electrons, giving rise to the amphoteric non-bridging oxygen (NBO) center (≡Si−O•) and the positively charged ≡Si^{+} center (known as the E'_s center). Collision of the secondary electron with one of the strained oxygen vacancy bonds, also concentrated near the interfaces, leads to the creation of the ≡Si^{+} •Si≡ center (known as the E'_γ center). Hole traps generated in the bulk of the oxide are shallow, while the centers distributed in the vicinity of the interfaces (NBO, E'_s, E'_γ) act as deep hole traps (Ristić et al., 2000).

Holes generated in the oxide by incident gamma radiation and through secondary ionization are far less mobile than the electrons. They are either trapped in the oxide, or move toward the floating gate under the influence of the electric field in the logic '1' state. Hole transport through the oxide occurs by means of two mechanisms: hopping transport via direct hole tunneling between localized trap sites, and trap-mediated valence band hole conduction. The holes not trapped in the oxide are injected into the floating gate, reduce the net amount of electron charge stored on it, and thereby decrease the threshold voltage of the cell's NMOS transistor. The trapping of holes occurs mostly at the oxide/floating gate interface, where the concentration of deep hole traps is high. The positive charge of these trapped holes, will tend to mask the negative electron charge on the floating gate, again reducing the transistor threshold voltage. Thus, the trapped and the injected holes both produce a negative threshold voltage shift.

Holes moving through the oxide cannot break unstrained silicon-oxygen bonds, but may create defects by interacting with either ≡Si−H or ≡Si−OH bonds, whereby hydrogen atoms and ions (H^o and H^+) are released. Once reaching the oxide/floating gate interface, holes can break both strained silicon-oxygen bonds and strained oxygen vacancy bonds, producing

NBO, E'_S and E'_γ centers. Holes trapped at the oxide/substrate interface which recombine with electrons injected from the substrate may produce another kind of amphoteric defect ($Si_3{\equiv}Si^{\bullet}$, a silicon atom at the interface back bonded to three silicon atoms from the floating gate) (Ristić et al., 2007).

Interface traps may also be generated through direct interaction of incident gamma photons. Another mechanism of interface trap buildup includes hydrogen atoms and ions released by the holes in the oxide. Hydrogen atoms and ions diffuse and drift toward the oxide/floating gate interface. When a H^+ ion arrives at the interface, it picks up an electron from the floating gate, becoming a highly reactive hydrogen atom H°, which is able to produce interface traps (Fleetwood, 1992).

Small oxide thickness gives rise to considerable fluctuation of absorbed energy, directly influencing the number of faults in the examined samples. Moreover, the amount of radiation-induced defects acting as electron and hole traps is a complex function of the gate oxide material, as well as of the doping and processing methods used in securing the oxide onto the silicon surface. These are the reasons for the observed variation in the number of faults among the examined memory samples.

Another effect caused by gamma radiation is electron emission from the floating gate. This kind of emission is the basis for standard EPROM erasure by UV radiation. During irradiation, gamma photons cause electrons to be emitted over the floating gate/oxide potential barrier. Once in the oxide, electrons are swept to the substrate or control gate by the electric field. The loss of electrons from the floating gate causes additional decrease of the threshold voltage.

The net effect of charge trapping in oxide and at oxide/floating gate interfaces, as well as of floating gate hole injection and electron emission, is the change of the NMOS transistor threshold voltage. Radiation induced change of the threshold voltage may affect memory cell logic state at readout. Threshold voltage V_T is, hence, the key parameter of memory cell state. Modeling charge stored at the NMOS floating gate as charge on a parallel plate capacitor, threshold voltage can be expressed as:

$$V_T = V_{T0} + \frac{q_s d}{\varepsilon} \tag{1}$$

where V_{T0} is the initial transistor threshold voltage, q_s is the gate surface charge density, d is the oxide thickness between the control and floating gate, ε is the oxide dielectric constant. This model disregards the dependence of threshold voltage on the actual position of the trapped charge sheet within the oxide. The influence of gamma irradiation on programmable memories is manifested through the change of the net gate surface charge density. Threshold voltage as a function of the absorbed dose can be represented by the empirical relation:

$$V_T(D) = V_T^{eq} + (V_{T0} - V_T^{eq})e^{-\alpha D} \tag{2}$$

where a is a constant dependent on the type and energy level density of the traps in the oxide, V_T^{eq} is the threshold voltage at extremely high doses, when an equilibrium of the three dominant processes contributing to the change of gate surface charge density - hole trapping, hole injection and electron emission - is achieved (Messenger & Ash, 1992).

The cumulative nature of gamma radiation effects observed in EPROM components can be attributed to the fact that no annealing of radiation induced interface states occurs at ambient temperature. Higher sensitivity of the tested EEPROM components to gamma radiation is a consequence of a more pronounced radiation induced electron emission from the floating gate over the thin oxide region (≈ 10 nm) between the floating gate and the drain (Wrobel, 1989).
UV photons with an energy lower than the bandgap of silicon dioxide (≈ 9 eV) are incapable of creating electron-hole pairs in the oxide, but are capable of exciting electrons from the silicon substrate into the oxide, where they recombine with the trapped holes. Irradiation of EPROMs by UV light during erasure partially reduces the radiation-induced trapped charge from previous exposure to gamma photons. This light-induced annealing of trapped holes can account for the observed reversibility of changes in EPROMs. Since EEPROM erasing process involves no UV irradiation, this effect is absent for these components. Thermal annealing of holes trapped at deep interface traps is not evident at ambient temperatures. Current-induced annealing of trapped holes, due to recombination of holes with electrons being driven from the floating gate to the drain, could be expected to occur during EEPROM electrical erasure. However, this kind of annealing is known to require much longer times compared to the duration of a standard EEPROM erasing procedure. On the whole, no significant annealing of trapped holes occurs in EEPROMs, and hence radiation-induced changes in these components appeared irreversible on the time scale of experiments performed in this paper (~ 10 hours) (Raymond, 1985).

3. Radiation hardness of over-voltage protection components

3.1 Theory

The power or signal lines over-voltage transients arise directly from the commutation process, electrostatic discharge, lightening stroke, or indirectly as a consequence of interaction between wire structures of the system and an electromagnetic field. An efficient over-voltage protection is highly important for reliable functioning of the protection equipment. Continous or temporary malfunctioning of the equipment caused by surge, could be a result of an improperly designed circuitry protection. Resistance to the occurrence of over-voltage is significantly reduced through miniaturization of electronic components. Therefore, more attention is paid to the protection of over-voltage components. This problem is particularly interesting when a fast electromagnetic pulse and radiation are simultaneously applied to the electronic components.
The over-voltage components could be generally divided into non-linear and linear components. Non-linear group includes the following: Transient Suppressers Diodes (TSD), Metal-oxide Varistors (MOV) and Gas Filled Surge Arresters (GFSA). Linear group of components includes capacitors, inductors, resistors or their combinations-filters.
The main disadvantage of linear over-voltage protection components is the frequency dependent protection efficiency. For all non-linear protective devices this is only a marginal problem - only at high frequencies may the protection efficiency of these devices suffer certain degradation (Lončar et al., 2005). Reliable operation of all electronic components (including over-voltage protection) at high temperatures is extremely important - particularly in a "mission critical" application. If the over-voltage protection is stabile and effective over a wide temperature range, it will significantly contribute to overall system reliability (Markov, 1987).

3.2 Experiment

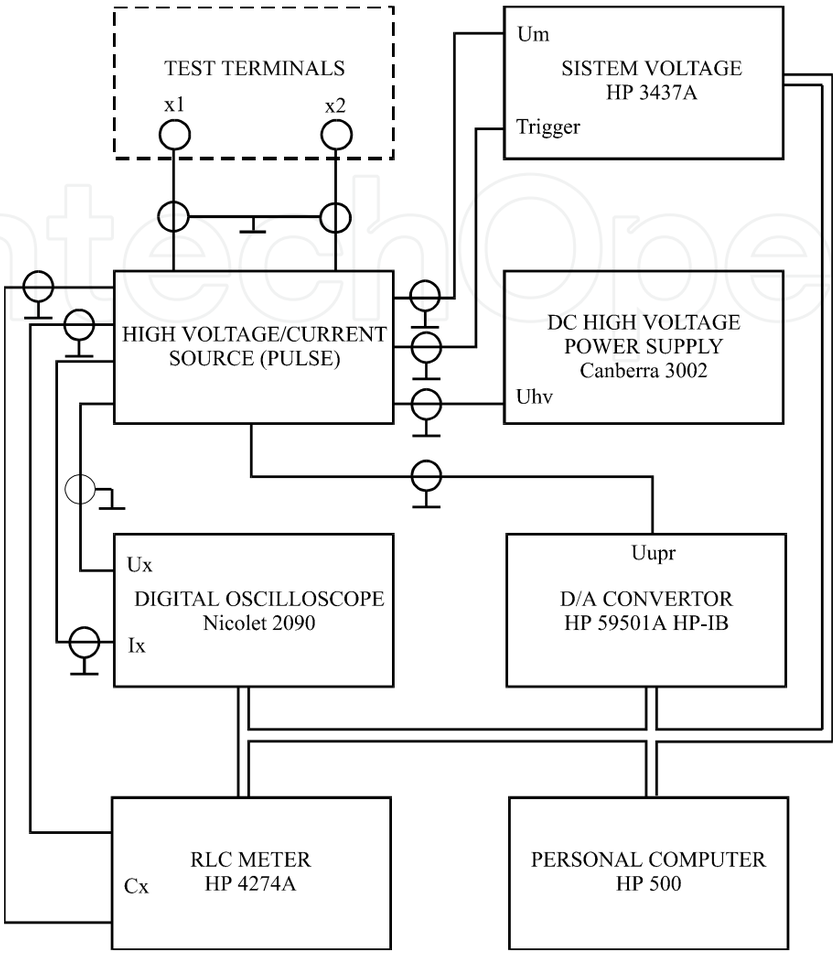

Fig. 4. Block scheme of measuring system

The examination of over-voltage protection components was carried out on the following commercial components:

1. Transient Suppresser Diodes (TSD) nominal voltage 250 V, maximum pulse current 1A;
2. Metaloxide Varistors (MOV) nominal voltage 230V, maximum impulse electric current 1200 A/ 2500 A;
3. Polycarbon Capacitors (nominal voltage 160 V, capacity 1μF);
4. Gas Filled Surge Arresters (GFSA) d.c. breakdown voltage 470V.

We examined the $n_{+}\gamma$ radiation from californium ^{252}Cf isotope influence on following characteristics of TSD and MOV:

1. volt-ampere characteristic;
2. volt-ohm characteristic;
3. nonlinear coefficient $\alpha = \log (I_2/I_1)/\log (U_2/U_1)$;
4. breakdown voltage.

The effects of $n_{+}\gamma$ radiation on following Polycarbon Capacitors characteristics were examined:

1. the dielectric loss factor, tg δ (measuring frequency f = 100 kHz);
2. capacitance, C (measuring frequency f = 100 kHz).

The effects of $n_{+}\gamma$ radiation on following GFSA characteristics were examined:

1. the random variable "pulse breakdown voltage";
2. the random variable "d.c. breakdown voltage";
3. the pulse shape (volt-second) characteristic.

Experiments were conducted using high voltage and measuring equipment consisting of current source, having the maximum voltage between terminals x_1 and x_2 of 3000 V, digital oscilloscope, D.C. high voltage power supply and personal computer, (Fig. 4.).

For TSD and MOV testing, the double exponential (8 x 20μs) current pulse method was applied. Double exponential voltage pulses (1,2 x 50μs) were applied in the GFSA and Polycarbon Capacitors testing. A random variable "D.C. breakdown voltage" test conducted on a GFSA consisted of 20 series each one having 50 measurements (1000 activation). Prior to experiments in each of the series, the element to be tested was conditioned with 25 breakdowns. A 30-second pause between two successive measurements was introduced. Polycarbon Capacitors were examined using the same measuring procedure used for impulse tests of GFSA. A RLC meter was used for this experiment.

All measuring instruments were protected from electromagnetic interference by electromagnetic shielding. The experimental procedure was fully automated. This approach assures very high accuracy of measurement and good repeatability of results. Specialized PC based control software (HP-IB or IEEE488 protocol) was developed to provide overall experiment sequencing, measurement and data acquisition (digital oscilloscope) and easy change of parameters (pulse modification - voltage and current source was generated using a D/A converter) (Osmokrović et al., 2006).

Table I and II present F_n and F_γ (neutron fluence and gamma flux respectively) dependencies versus N_F (the exposure number) for TSD & MOV and Polycarbon Capacitors, respectively.

N_F	$Fn(n/cm^2)\cdot 10^{10}$	$F\gamma(\gamma/cm^2)\cdot 10^{13}$
0	0	0
1	3.55	8.66
2	7.10	17.3
3	10.66	26

Table 1. Values for neutron fluence (F_N) and gamma flux (F_γ) versus N_F (the exposure number) for TSD and MOV

N_F	$Fn(n/cm^2)\cdot 10^{10}$	$F\gamma(\gamma/cm^2)\cdot 10^{13}$
0	0	0
1	2.79	6.8
2	5.59	13.6
3	8.37	20.4

Table 2. Values for neutron fluence (F_N) and gamma flux (F_γ) versus N_F (the exposure number) for Polycarbon Capacitors

3.3 Results and discussion

3.3.1 Radiation hardness of TSD

In Figures 5 (a)-(d) volt-ampere, volt-ohm, breakdown voltage and the nonlinear coefficient versus $n_{+}\gamma$ fluence/flux characteristics are shown respectively (Vujisić b et al., 2007).

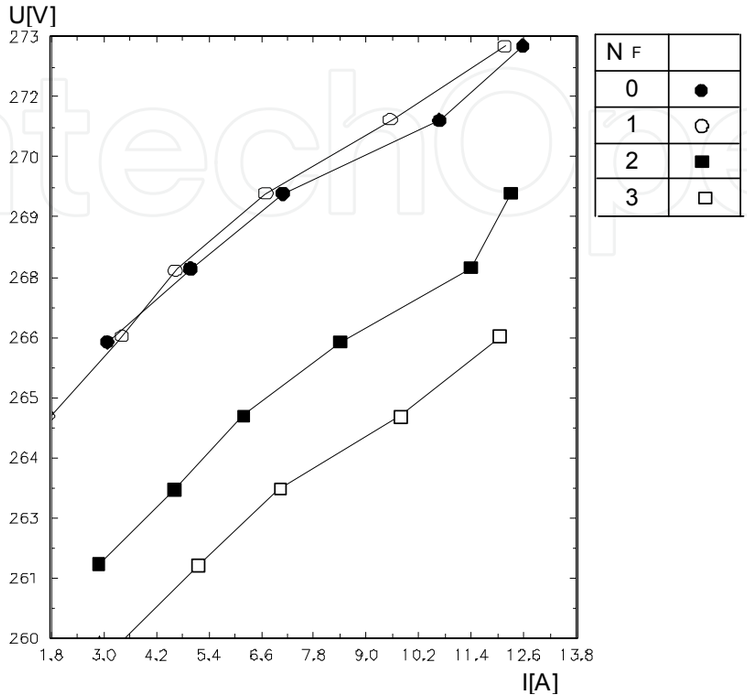

Fig. 5(a). The TSD volt-ampere versus $n_{+}\gamma$ fluence / flux characteristic

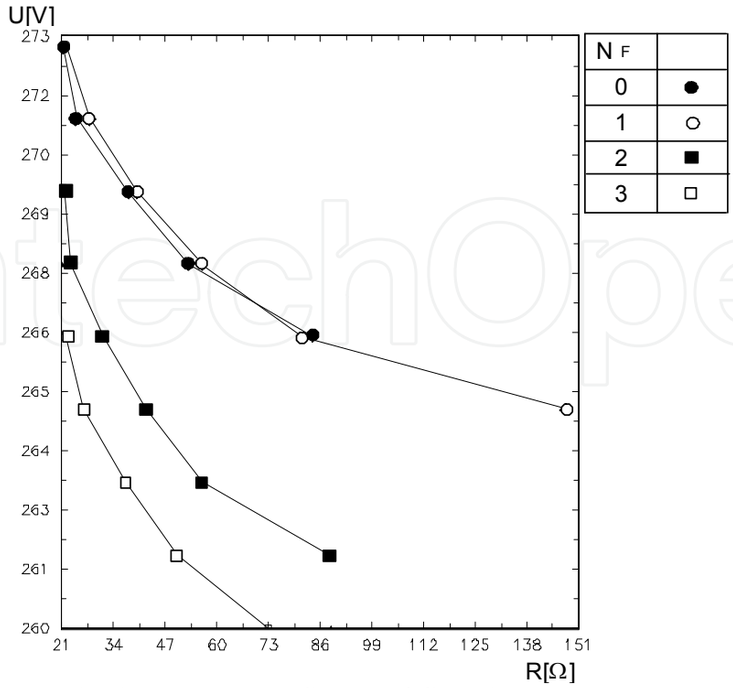

Fig. 5(b). The TSD volt-ohm versus $n_{+}\gamma$ fluence / flux characteristics

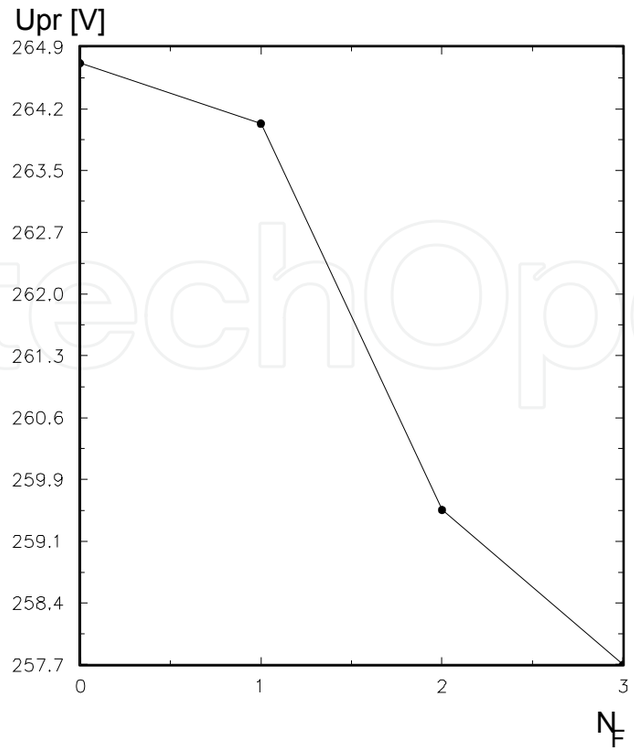

Fig. 5(c). The TSD breakdown voltage versus $n_{+}\gamma$ fluence / flux characteristics

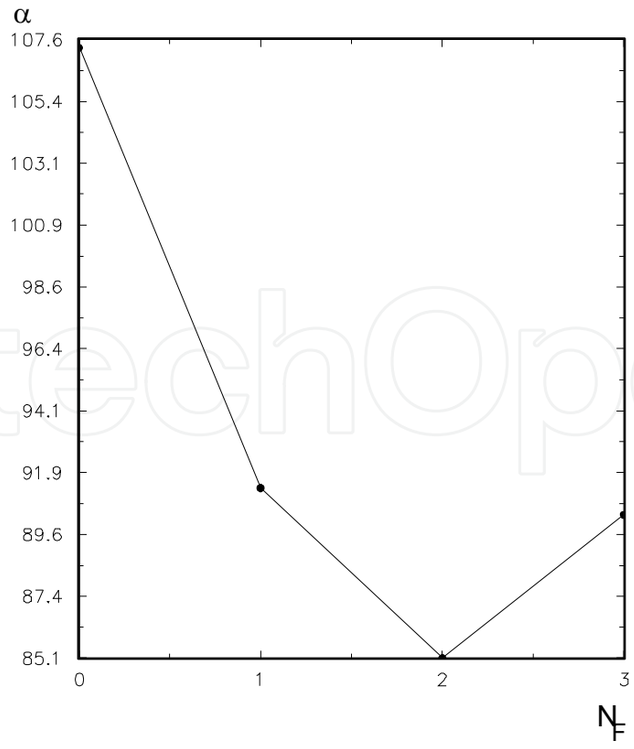

Fig. 5(d). The TSD nonlinear coefficient versus $n_{+}\gamma$ fluence / flux characteristics

According to these diagrams TSD exhibits breakdown voltage drop, due to increase of the volt-ampere slope, and consequently decrease of non-linear coefficient.
The changes which were noticed could be explained by irreversible TSD material changes caused by $n_{+}\gamma$ radiation. This radiation influences generation different radiation defects which directly causes degradation of electric characteristics of over - voltage protection components (life time, minority charge carrier concentrations, mobility, specific resistance). The most typical radiation defect for applied doses is Frenkel (Van Lint et al., 1980). The energy levels of these defects are located inside the energy gap. Although minority charge carriers life time is determined by bulk recombination velocity at traps and local centers, recombination efficiency, e.g. minority charge carriers life time depends on traps concentration and probability of minority charge carriers trapping by recombination centers. For this reason these defects represent very efficient recombination centers. Consequently, recombination likelihood becomes higher, which decreases minority charge carrier's life time. Thus, TSD Reverse Current becomes larger which causes breakdown voltage drop. Tested TSD has relatively high voltage protection element (250V), therefore relatively small radiation doses caused significant breakdown voltage drop (Fig. 5c) (approximately 50 %).
Second radiation effect is related to minority charge carriers mobility and concentration decrease which causes increase of specific resistance of the initial semiconductor material. Thus, TSD material exhibits specific resistance increase. Consequently, nonlinear coefficient decreases worse and the TSD protection characteristics degrades. Influence of radiation neutron components on degradation of TSD protection characteristics is much larger then influence of γ component. It is noticed that one displacement of atoms from silicon crystal lattice under influence of γ photons with energy of 1,5 MeV causes 140 displacements under influence of same energy neutrons. On other hand that ratio is 2,7 by γ photon, e.g. 150 by neutrons at energy of 120 MeV. This shows that contribution of γ radiation effects to displacement is negligible to that of neutron radiation effects (Holmes- Siedle & Adams, 2002).

3.3.2 Radiation hardness of MOV

In Fig. 6(a)-(d) the MOV volt-ampere, volt-ohm, breakdown voltage and nonlinear coefficient versus $n_{+}\gamma$ fluence/flux characteristics are represented, respectively.
According to diagrams, MOV exhibits breakdown voltage drop due to increase of the volt-ampere slope and consequently decrease of nonlinear coefficient.
Generally, metaloxide varistors exhibits more pronounced protection characteristics degradation compared to TSD.
The obtained results are not in full agreement with the expected ones (Malinarić, 1985). Therefore, the experiments are performed a number of times in strictly controlled conditions with high rate of reliability and repeatability and every time with same results.
Therefore, appearance of dislocation in metaloxide varistor structure does not change carrier life time, so larger influence of $n_{+}\gamma$ radiation on metaloxide varistor characteristics (volt - ampere, volt -ohm, breakdown voltage and nonlinear coefficient) is not expected. But, experimental results show significant influence of $n_{+}\gamma$ radiation on degradation of metaloxide varistor characteristics. These results could be explained by dislocation capturing charge carriers, which causes decrease of free charge carriers. These further leads to decrease of metaloxide varistors specific conductivity and to increase of local electric

field nearby dislocations (Mahan et al., 1979). Decrease of specific conductivity explains volt - ampere and volt - ohm curves. On the other hand decrease of breakdown voltage is explained by increase of local electric fields.

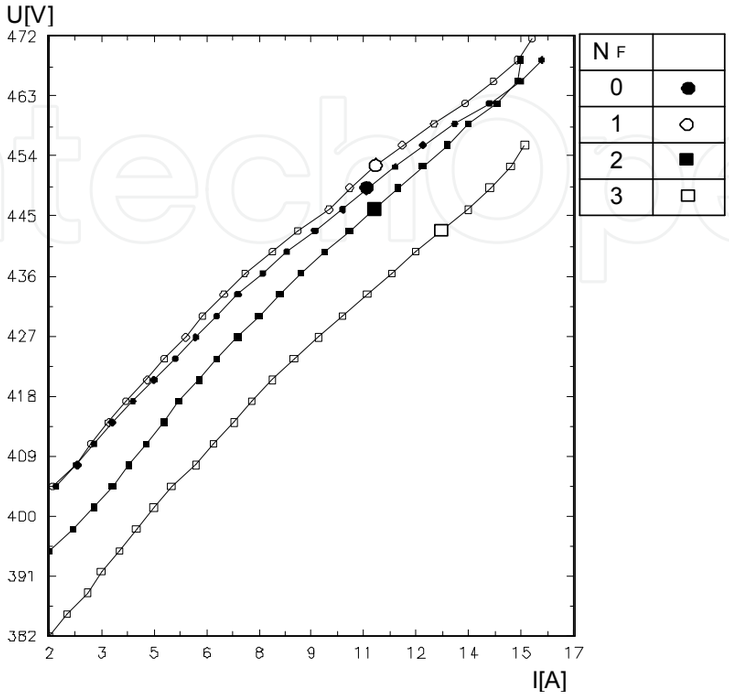

Fig. 6(a). MOV volt-ampere versus $n_{+}\gamma$ fluence / flux characteristics

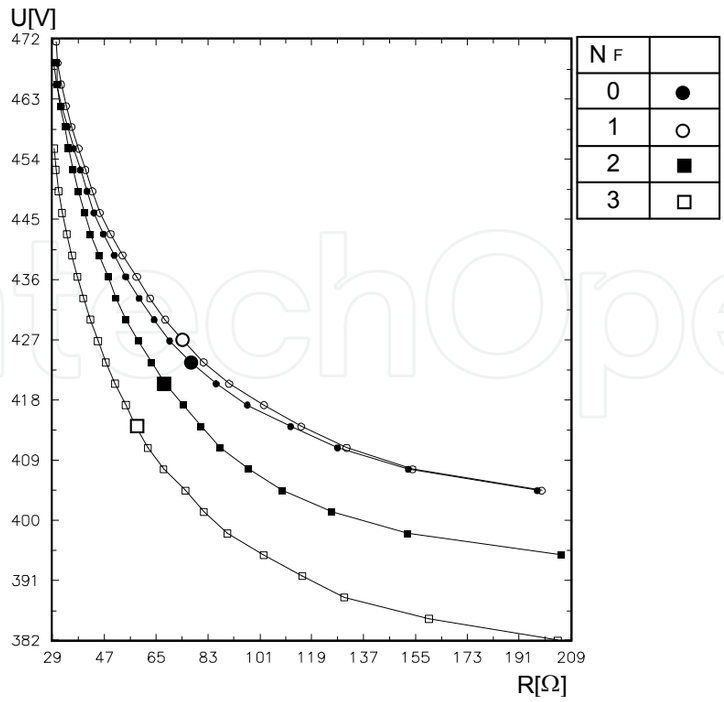

Fig. 6(b). MOV volt-ohm versus $n_{+}\gamma$ fluence / flux characteristics

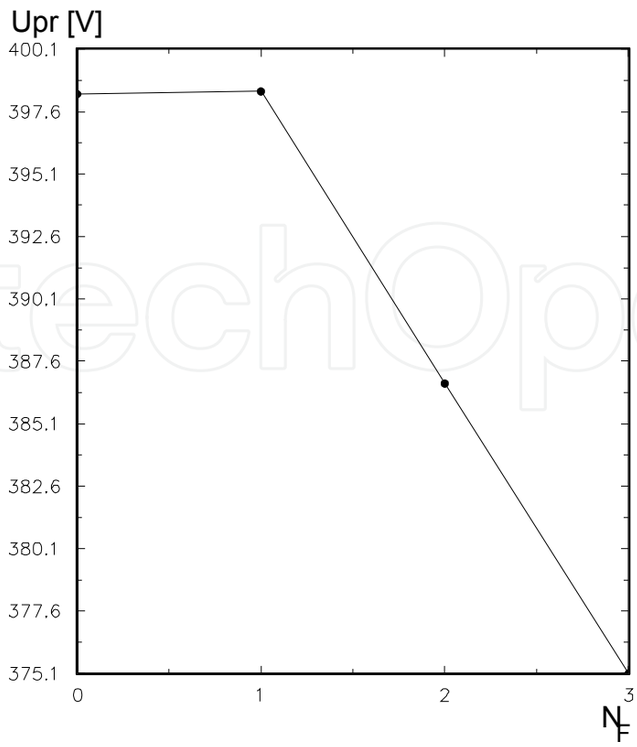

Fig. 6(c). MOV breakdown voltage versus $n_{+}\gamma$ fluence/ flux characteristics

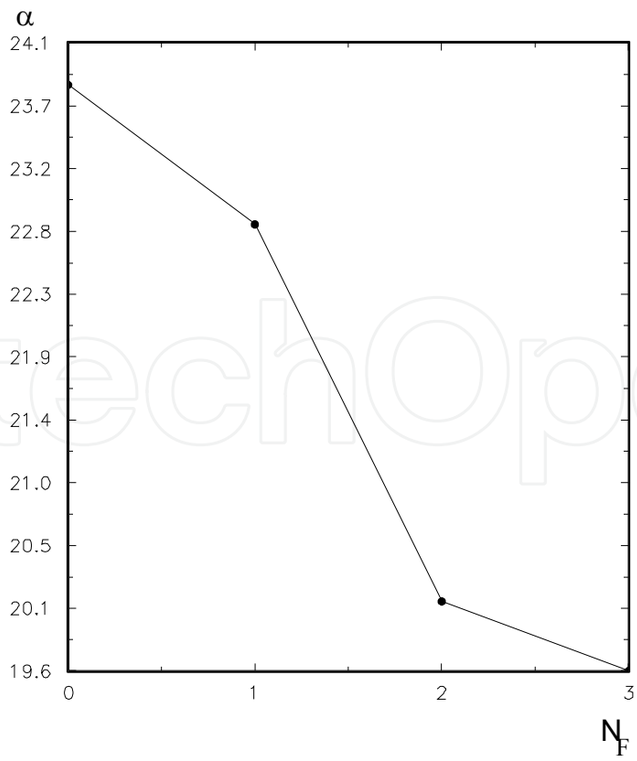

Fig. 6(d). MOV nonlinear coefficient versus $n_{+}\gamma$ fluence / flux characteristics

Irreversible changes of electric characteristics of metaloxide varistors are caused by inelastic interactions with atom material nucleus. Since the cross section of inelastic interaction of neutron component is larger than corresponding γ component noticed effect is mostly result of neutron component radiation (Messenger & Ash, 1992).

3.3.3 Radiation hardness of polycarbonate capacitors

In Fig. 7 the change in the capacity of polycarbon capacitors versus $n_+\gamma$ fluence/flux radiation is depicted. Examined capacitor has a very high insulated degree (10 -100 TΩ) and small losses (tgδ = 0,0015). During examination a measurable influence of $n_+\gamma$ radiation on the loss factor tgδ was not found. According to this diagram we can conclude that radiation causes a decrease in the capacity of capacitors. After repeating this experiment in 120 hours, effects of reversible nature were noticed (Lončar et al., 2007).

Influence of neutron and γ radiation on polycarbonat can be observed in two phases. As a result of first phase ionizing radiation free electrons, positive ions and excess molecules are formed. In second phase free radicals are formed. Huge amount of free radicals in polymer leads to irreversible changes which is consist of destruction processes and structure changes. Destruction is process of breaking main chains of connected macro molecules which causes molecule mass drop and gas occurring. Destruction mechanism is determined by individual characteristics of radiated material. Nowadays, for larger number of polymers destruction process is not well known to the end. It should be noticed that small radiation doses can change physical characteristics of polymer materials (Clegg & Collyer, 1991).

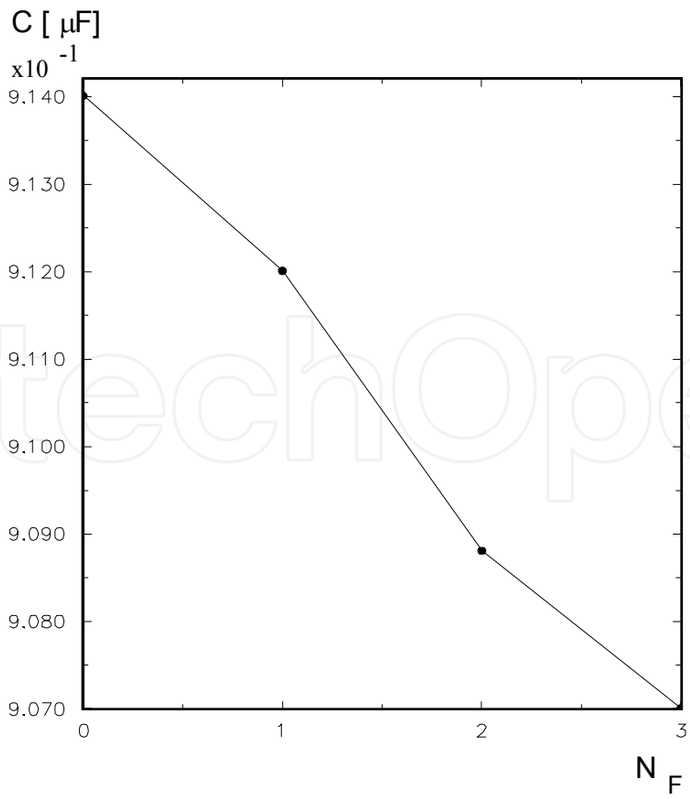

Fig. 7. Polycarbon capacitor value versus $n_+\gamma$ fluens/ flux characteristics

The decrease of capacitors capacity when under the radiation of $n+\gamma$ flux can be explained by forming the ionized structure inside the dielectric volume. Those structures influence the partial screening of the electric field in the capacitors. Greater number of ions appearing in dielectric initiate higher influence of ion type polarization on dielectric constant of material. This leads to decrease of capacity. Also, ion pairs by there local field partially screening external electric field (Gromov & Evdokinov, 1984). Still the change in the capacitance of the capacitors caused by it is relatively small. The existence of these structures in the dielectric leads to its aging and to the decrease of the breakdown voltage . The reversibility of these phenomena is a result of recombination processes. This shows that the doses of radiation were not high enough to cause significant changes in the molecular structure of the dielectric.

3.3.4 Radiation hardness of GFSA

3.3.4.1 The effect of induced radiation

A GFSA dc breakdown voltage versus neutron fluence dependence is presented in Fig. 8. Fig. 9 present the GFSA pulse shape characteristics before and after the exposure to the radioactive source (Lončar et al., 2003).

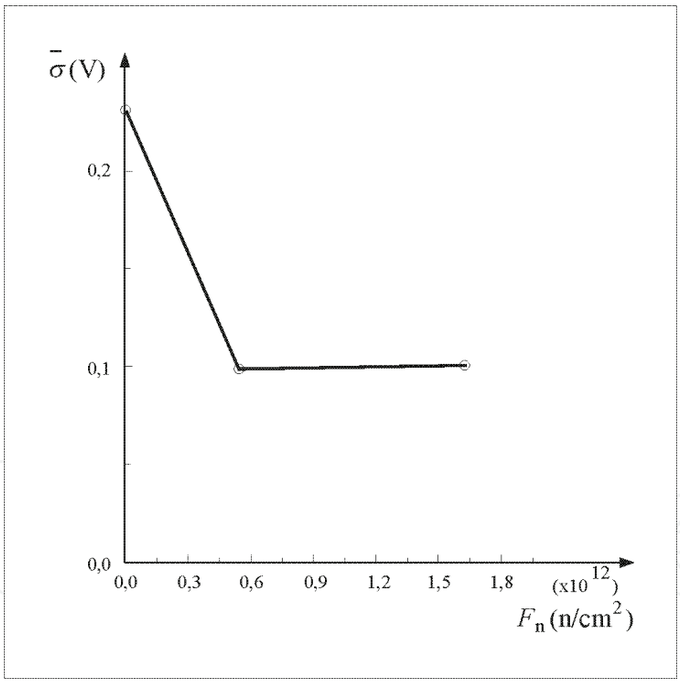

Fig. 8. The GFSA dc breakdown voltage versus neutron fluence characteristic

Since cross section for capturing neutrons has large enough value only for thermal and slow neutrons and due to structure of californium source fission spectra relatively small part of neutrons takes part in activation of GFSA material (Messenger & Ash, 1992). Besides this restriction as a result of GFSA radiation a change of its electrical characteristics was noticed. GFSA was influenced by neutron fluence of 5,4148 x 10^9 n/cm^2 same as neutron fluence of 16,244 x 10^{11} n/cm^2. Although, except the neutron component part of radiation was also γ

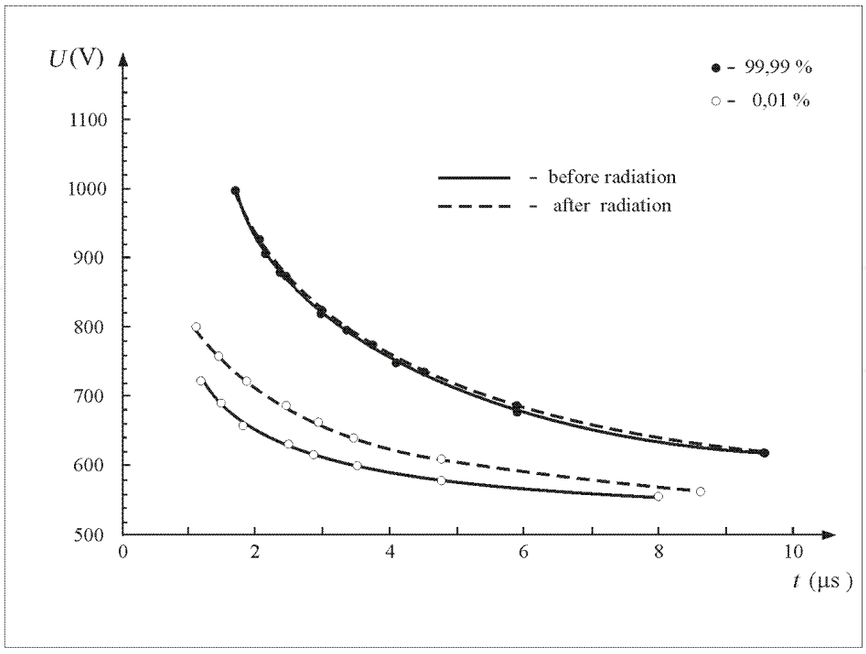

Fig. 9. The GFSA pulse shape characteristic

component, which can influence only changes of electric characteristics of GFSA until its displace from field of radiation. It means that we can observe effects of radiation of GFSA only as influence of neutron fluence.

The obtained results show that after irradiating GFSA the standard deviation of the static breakdown voltage is significantly decreased. The pulse voltage tested GFSA shows that the irradiated GFSA acts more readily and has somewhat narrower voltage-time characteristic than unirradiated GFSA. In other words it had a smaller discharge value of dc breakdown voltage (Fig.10) (1,84% and before radiation 3,11%). This means that its protective characteristics are improved.

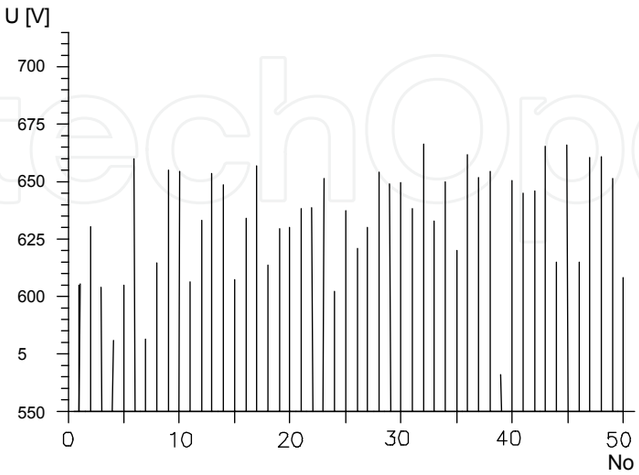

Fig. 10(a). Chronological series of measured values of GFSA d.c. Breakdown Voltage before radiation

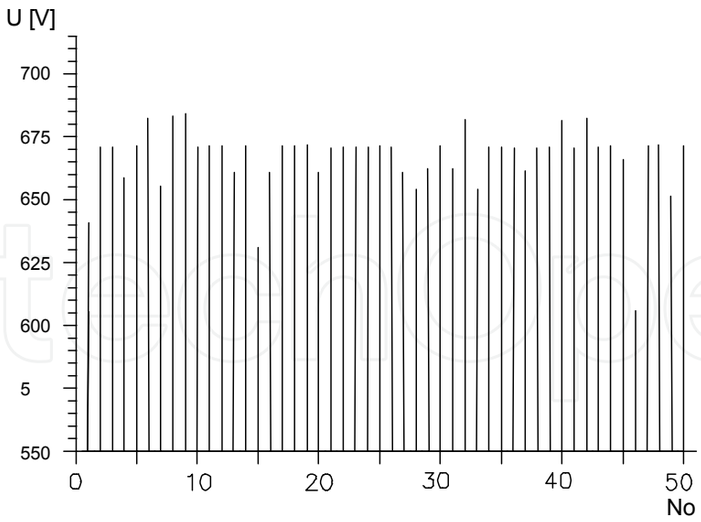

Fig. 10(b). Chronological series of measured values of GFSA d.c. Breakdown Voltage immediately after radiation

A faster response of an irradiated GFSA was the consequence of the higher concentration of free electrons in the inter-electrode gap stimulated by a gas ionization. This ionization was induced by neutron activation of a GFSA material. Faster response time of GFSA can be explained as a consequence of the increased availability of free electrons that caused a statistic time decrease.

Figures 11(a) and 11(b) present the GFSA activation analysis diagrams immediately after the exposure to the radioactive source and six hours after radiation effects obtained by γ-ray

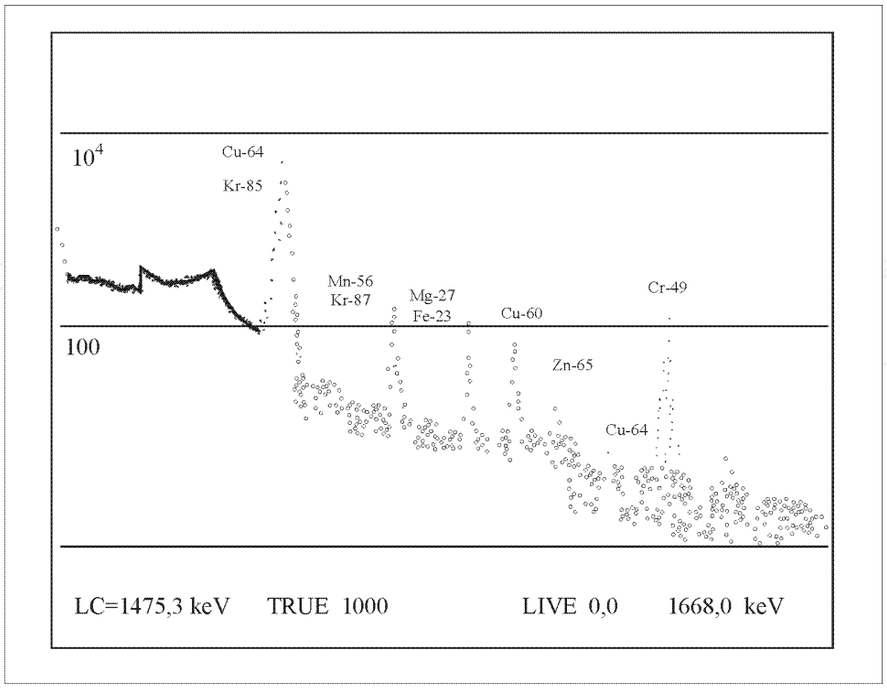

Fig. 11(a). Diagram of the GFSA activation analysis immediately after radiation effects

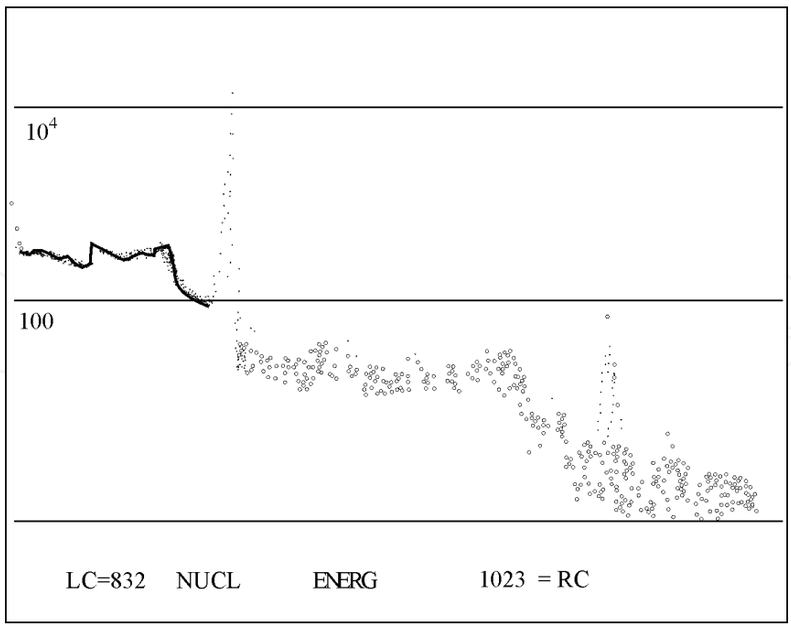

Fig. 11(b). Diagram of the GFSA activation analysis six hours after radiation effects

spectrometer, respectively. Identified radioactive isotopes are recorded close to the expected energy peaks. The activity of these isotopes consists of both γ and β component. Due to the induced radioactivity, the gas ionization is intensified and the statistical time of a pulse breakdown voltage is reduced. Neutron radiation effects improve the pulse shape characteristic for a short period of time. This effect of neutron radiation disappears quickly, as the half-life time of induced activity varies from several minutes to several hours. This fact is confirmed clearly in the diagram for the activation analysis of radiated GFSA taken after six hours (Fig. 11(b)). From these diagrams one notices, that neutron activation products have completely decayed and the device GFSA had recovered back to the unirradiated state.

3.3.4.2 The effect of built-in radiation

In GFSA model α and β sources were built-in. ^{241}Am used as an α-emitter in experiment has the activity of 1735 Bq with the energy of 5485.6 keV and the activity of 267 Bq with the energy of 5442.9 keV. As a β-emitter ^{90}Sr -^{90}Y source was used (first continuous spectrum from ^{90}Sr has a total average of β- energy of 196 keV and the maximum energy of β electrons as highest energy in energy range from endpoint of internal Bremsstrahlung 546 keV, second continuous spectra from ^{90}Y has total average β- energy 934 keV and maximum energy of β electrons as the highest energy in the energy range from the endpoint of internal Bremsstrahlung 2282 keV). In order to get a detailed insight into how the radiation influences the GFSA characteristics, the types of gas and its pressure were varied.
In Fig. 12, the GFSA dc breakdown voltage versus a variable 'pd' (p is the gas pressure in the chamber, d is the interelectrode gap) is presented before the radiation and with a built-in α and β radioactive sources. In Fig. 13, GFSA voltage-time characteristics with built-in α and with built-in β radioactive sources are given (Osmokrović a et al., 2002).
On the basis of the experimental results we can conclude that built-in radioactive sources significantly improve the protective characteristics of GFSA. This is especially obvious in the

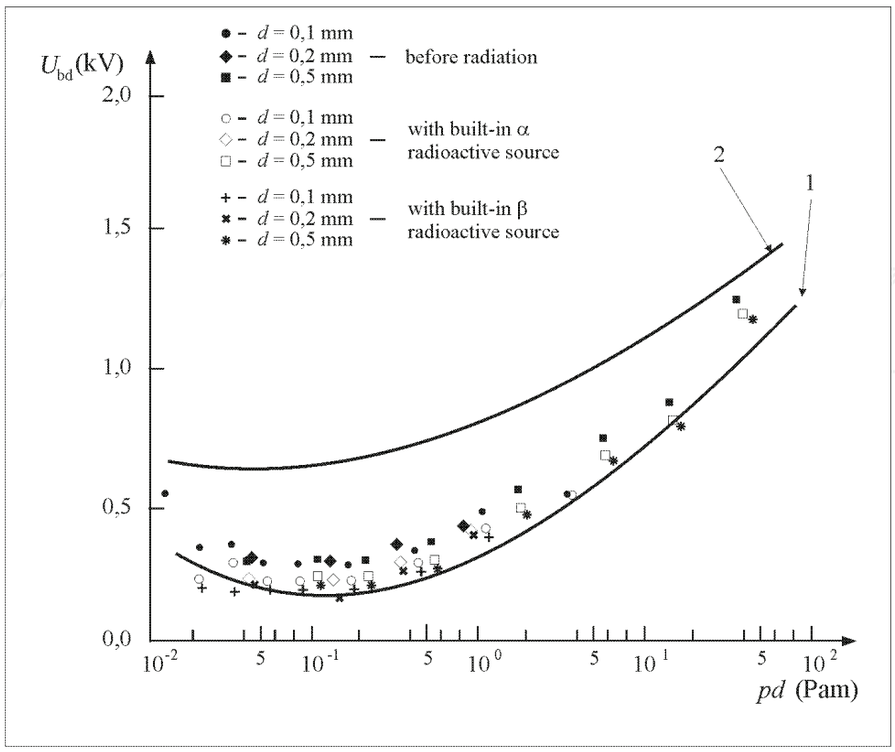

Fig. 12. The GFSA dc breakdown voltage versus variable pd before radiation, with built-in α and with built-in β radioactive source (p is Argon gas pressure in the chamber, d is interelectrode gap) Curve 1- Townsend breakdown mechanism, Curve 2- Streamer breakdown mechanism

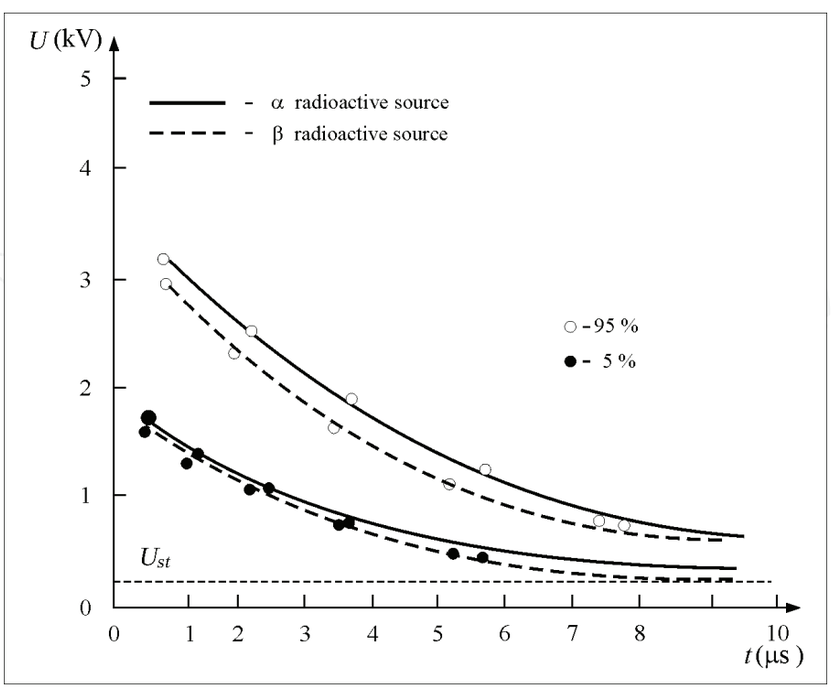

Fig. 13. The GFSA pulse shape characteristic with built-in α and β radioactive source

decrease of the response time by more than three times compared to that without radioactive sources (e.g. from 100 ns to 30 ns). At lower pressures (10^2 Pa – 10^3 Pa) it is more effective to use the α-emitters while at the higher pressures (10^5 Pa – 10^6 Pa) the β-emitters has proved to be more effective because of the greater cross section for ionization by β-particles (Osmokrović et al., 2005).

4. Conclusion

This text presents the results of the examination of programmable memories' radiation reliability. Influence of cobalt-60 gamma radiation was tested on NM27C512 8F85 EPROM and M24128 - B W BN 5 T P EEPROM components. EPROM components proved to have better radiation reliability than EEPROMs. Significant faults in EPROM and EEPROM components appeared at 1300 Gy and 1000 Gy, respectively. Changes in EPROMs are reversible, and after erasing and reprogramming, all EPROM components are functional. Reversibility of changes in EPROMs is attributed to partial light-induced annealing of trapped holes during UV erasure. Due to the cumulative radiation effects, first failures of the previously irradiated EPROMs appear at significantly lower doses. On the other hand, EEPROM changes are irreversible. All observed phenomena have a plausible theoretical explanation, based on the interaction of gamma radiation with the oxide layer of memory cell MOS transistors. The influence of gamma radiation is basically manifested through the change of the net gate surface charge density, and consequently of transistor threshold voltage.

For future work we planned the following:

1. To investigate these results for other EPROM and EEPROM components;
2. To include the gate insulator material and its thickness in research;
3. To consider the processing and doping methods used in securing the gate insulator onto the silicon surface;
4. To investigate the radiation-induced mobility changes;
5. To examine the dose rate effects;
6. To investigate the temperature influence of the memory during irradiation.

Also, in this chapter the examination of radiation resistance results of the components of over-voltage protections were presented. The influence of $n_+\gamma$ radiation was tested on the TSD, MOV, GFSA and Polycarbon Capacitors (the most sensitive elements of the electric filter).

It was concluded that under $n_+\gamma$ radiation the protection characteristics of TSD degrades considerably worse. A similar effect, only more pronounced was noticed in the case of the MOV. In the case of GFSA, the protection characteristics were improved under $n_+\gamma$ radiation. Polycarbon Capacitors exposed to $n_+\gamma$ radiation in a given fluence range, under goes a change in its capacitance towards smaller values.

These results show that TSD, MOV and Polycarbon Capacitors are radiation sensitive components. The GFSA shows a considerable improvement of the protection characteristics under $n_+\gamma$ radiation. Therefore by investigating the obtained results, it can be noticed that GFSA shows the best characteristics stability under radiation influence, among examined over - voltage protection components. The results obtained when GFSA is in a radiation environment, show that there is no need to use GFSA with built-in radioactive sources,

because the induced radiation causes the same or a very similar effect. This conclusion is very important from both the environment protection and the GFSA production point of view. Moreover, using short living radioactive isotopes, it is possible to produce faster GFSA. After a certain period of time, the GFSA would lose their characteristics, so their storage and disposal would not cause any more risk to the environment. We believe that future experiments should be directed towards the investigation of the possibility of a combined use of short lived radioactive isotopes and the hollow cathode effect.

It means that in conditions of increased hazardous radiation GFSA gives the best protection. Of course it doesn't mean that other over - voltage protection elements are not more reliable in some other hales (temperature (Lončar et al., 2002), electromagnetic contamination, aging (Osmokrović b et al., 2002), dimension, price). However, if several factors influence the devices simultaneously, hybrid protective scheme should be employed, which includes different types of over - voltage protection elements.

5. References

Clegg, D. W. & Collyer, A. A. (1991). *Irradiation Effects on Polymers,* Kluwer Academic Publishers, New York

Fleetwood, D. M. (1992). Border Traps in MOS Devices. *IEEE Trans. Nucl. Sci.*, Vol. 39, No. 2, 269–271

Gromov, V.V. & Evdokimov, O.B. (1984). *Trapping Charge Phenomena In Irradiated Dielectrics*, Pergamon Press, New York

Holmes – Siedle, A. & Adams, L. (2002). *Handbook of Radiation Effects*, Oxford University Press, Oxford

Hubbell, J. H. & Seltzer, S.M. (2004). *Tables of X-Ray Mass Attenuation Coefficients and Mass Energy-Absorption Coefficients* (version 1.4), National Institute of Standards and Technology, Gaithersburg, MD. Available Online: http://physics.nist.gov/xaamdi

Lončar B., Osmokrović P., Stojanović M., & Stanković S. (2001). Radioactive Reliability of Programmable Memories, *Jpn. J.Appl. Phys*., Vol. 40 Pt. 1, No. 2B, 1126 –1129.

Lončar B., Osmokrović P. & Stanković S. (2002). Temperature Stability of Components for Over-voltage Protection of Low-voltage Systems, *IEEE Trans. Plasma Sci*., Vol. 30, No. 5, 1881-1885.

Lončar B., Osmokrović P. & Stanković S. (2003). Radioactive Reliability of Gas Filled Surge Arresters, *IEEE Trans. Nucl. Sci*., Vol. 50, No. 5, 1725–1731

Lončar B., Stanković S., Vasić A. & Osmokrović P. (2005). The Influence of Gamma and X-radiation on Pre-breakdown Currents and Resistance of Commercial Gas Filled Surge Arresters, *Nucl. Tech. & Rad. Prot*., Vol. 20, No. 1, 59-63.

Lončar B., Osmokrović P.; Vujisić M. & Vasić A. (2007). Temperature and Radiation Hardness of Polycarbonate Capacitors, *J. Opt.* & *Adv. Mat.*, Vol. 9, No. 9, 2863-2866

Ma, T. P. & Dressendorfer, P.V. (1989). *Ionizing Radiation Effects in MOS Devices and Circuits*, John Wiley & Sons, New York

Mahan, C. D.; Levinson, L. M. & Philipp, H. R. (1989). Theory of Conduction in ZnO Varistors. *Journal of Applied Physics*, Vol. 50, No. 4, 424-428

Malinaric, P. (1985). Transient Suppressor Design with Varistor Composite Materials. *IEEE Trans. Electromagnetic Compatability*, Vol. 23, No. 4, 338-343

Markov, Z. (1987). *Over-voltage Protection in Electronics and Telecommunications*, Technical book, Belgrade, Yugoslavia

Messenger, G.C. & Ash, M.S. (1992). *The Effects of Radiation on Electronic Systems*, Van Nostrand Reinhold, New York

Osmokrović P.; Lončar B. & Stanković S. (2002). Investigation the Optimal Method for Improvement the Protective Characteristics of Gas Filled Surge Arresters-with/without the Built in Radioactive Sources, *IEEE Trans. Plasma Sci.*, Vol. 30, No. 5, 1876-1880.

Osmokrović P.; Lončar B., Stanković S. & Vasić A. (2002). Aging of the Over-voltage Protection Elements Caused by Over-Voltages, *Microel. Rel.*, Vol. 42, No. 12, 1959 1966.

Osmokrović P.; Lončar B. & Šašić R. (2005). Influence of the Electrode Parameters on Pulse Shape Characteristic of Gas-filled Surge Arresters at small Pressure and Inter-electrode Gap Values, *IEEE Trans. Plasma Sci.*, Vol. 33, No. 5, 1729-1735.

Osmokrović P.; Lončar B. & Stanković S. (2006). The New Method of Determining Characteristics of Elements for Overvoltage Protection of Low-voltage System, *IEEE Trans. Instr. & Meas.*, Vol. 55, No. 1, 257-265.

Prince, B. (1991). *Semiconductor Memories*, *A Handbook of Design, Manufacture and Applications*, John Wiley & Sons, New York

Raymond, J. P. (1985). IEEE Nuclear and Space Radiation Effects Short Course Notes, *Proceedings of Nuclear and Space Radiation Effects Conference,* pp. 5-15, New York, July 1985, New York

Ristić, G. S.; Pejović M. M. & Jaksić A. B., (1998). Modelling of Kinetics of Creation and Passivation of Interface Traps in Metal-oxide-semiconductor Transistors during Postirradiation Annealing, *J. Appl. Phys.*, Vol. 83, No. 6, 2994–3000

Ristić, G. S.; Pejović M. M. & Jakšić A. B., (2000). Analysis of Postirradiation Annealing of *n*-channel

Power Vertical Double-diffused Metal-oxide-semiconductor Transistors. *J. Appl. Phys.*, Vol. 87, No. 7, 3468–3477

Ristić, G. S.; Pejović M. M. & Jakšić A. B., (2007). Physico-chemical Processes in Metal-oxide-semiconductor Transistors with Thick Gate Oxide during High Electric Field Stress, *J. Non-Cryst. Sol.*, Vol. 353, 170–179

Snyder, E. S.; McWhorter P. J.; Dellin T.A. & Sweetman J. D. (1989). Radiation Response of Floating Gate EEPROM Memory Cells, *IEEE Trans. Nucl. Sci.*, Vol. 36, No. 6, 2131–2139

Srour, J.R. (1982). *Basic Mechanisms of Radiation Effects on Electronic Materials, Devices and Integrated Circuits,* DNA-TR-82-20, New York.

Van Lint, V. A. J.; Flanagan, T. M.; Leadon, R.E. & Rogers, C. V. (1980) *Mechanisms of Radiation Effects in Electronic Materials*, John Wiley & Sons, New York

Vujisić M.; Osmokrović P.; & Lončar B. (2007). Gamma irradiation effects in programmable read only memories, *J. Phys. D: Appl. Phys.*, Vol. 40, 5785–5789

Vujisić M.; Osmokrović P.; Stanković K.; & Lončar B. (2007). Influence of Working Conditions on Over-voltage Diode Operations, *J. Opt.* & *Adv. Mat.*, Vol. 9, No. 12, 3881-3884

Wrobel, T. F. (1989). Radiation Characterization of a 28C256 EEPROM. *IEEE Trans. Nucl. Sci.*, Vol. 36, No. 6, 2247–2251

Micro Electronic and Mechanical Systems

Edited by Kenichi Takahata

ISBN 978-953-307-027-8

Hard cover, 386 pages

Publisher InTech

Published online 01, December, 2009

Published in print edition December, 2009

This book discusses key aspects of MEMS technology areas, organized in twenty-seven chapters that present the latest research developments in micro electronic and mechanical systems. The book addresses a wide range of fundamental and practical issues related to MEMS, advanced metal-oxide-semiconductor (MOS) and complementary MOS (CMOS) devices, SoC technology, integrated circuit testing and verification, and other important topics in the field. Several chapters cover state-of-the-art microfabrication techniques and materials as enabling technologies for the microsystems. Reliability issues concerning both electronic and mechanical aspects of these devices and systems are also addressed in various chapters.

InTech Europe
University Campus STeP Ri
Slavka Krautzeka 83/A
51000 Rijeka, Croatia
Phone: +385 (51) 770 447
Fax: +385 (51) 686 166
www.intechopen.com

InTech China
Unit 405, Office Block, Hotel Equatorial Shanghai
No.65, Yan An Road (West), Shanghai, 200040, China
中国上海市延安西路65号上海国际贵都大饭店办公楼405单元
Phone: +86-21-62489820
Fax: +86-21-62489821

IntechOpen